Aesth Plast Surg (2017) 41:1228–1236
DOI 10.1007/s00266-017-0900-5

ORIGINAL ARTICLE BASIC SCIENCE/EXPERIMENTAL

Robot-Assisted Surgery for Mandibular Angle Split Osteotomy Using Augmented Reality: Preliminary Results on Clinical Animal Experiment

Chaozheng Zhou[1] · Ming Zhu[2] · Yunyong Shi[3] · Li Lin[2] · Gang Chai[2] · Yan Zhang[2] · Le Xie[4]

Received: 10 February 2017 / Accepted: 5 May 2017 / Published online: 19 July 2017

Abstract Mandibular angle split osteotomy (MASO) is a procedure widely used for prominent mandibular angles. However, conventional mandibular plastic surgery is invasive and high risk. It may induce postoperative neurosensory disturbance of the inferior alveolar nerve, fractures and infection due to the complexity of the anatomical structure and the narrow surgical field of view. The success rate of MASO surgery usually depends on the clinical experience and skills of the surgeon. To evaluate the performance of inexperienced plastic surgeons conducting this surgery, a self-developed and constructed robot system based on augmented reality is used. This robot system provides for sufficient accuracy and safety within the clinical environment. To evaluate the accuracy and safety of MASO surgery, an animal study using this robot was performed in the clinical room, and the results were then evaluated. Four osteotomy planes were successfully performed on two dogs; that is, twenty tunnels (each dog drilled on bilaterally) were drilled in the dogs' mandible bones. Errors at entrance and target points were 1.04 ± 0.19 and 1.22 ± 0.24 mm, respectively. The angular error between the planned and drilled tunnels was $6.69° \pm 1.05°$. None of the dogs experienced severe complications. Therefore, this technique can be regarded as a useful approach for training inexperienced plastic surgeons on the various aspects of plastic surgery.
No Level Assigned This journal requires that authors assign a level of evidence to each article. For a full description of these Evidence-Based Medicine ratings, please refer to the Table of Contents or the online Instructions to Authors www.springer.com/00266.

Keywords Mandibular angle split osteotomy · Augmented reality · Robot surgery · Osteotomy plane

Chaozheng Zhou and Ming Zhu have contributed equally to this paper.
Dr. Yan Zhang also contributes equally with Prof. Le Xie as corresponding authors.

✉ Gang Chai
13918218178@163.com

✉ Yan Zhang
13651817522@163.com

✉ Le Xie
lexie@sjtu.edu.cn

Chaozheng Zhou
zhouczg2008@126.com

Ming Zhu
drmingzhu@hotmail.com

Yunyong Shi
shi-yun-yong@163.com

Li Lin
330747210@qq.com

[1] Institute of Forming Technology and Equipment, Shanghai Jiao Tong University, Xuhui, Shanghai 200030, China

[2] Department of Plastic and Reconstructive Surgery, Shanghai 9th People's Hospital, Shanghai Jiao Tong University School of Medicine Shanghai, Huangpu, Shanghai 200011, China

[3] School of Biomedical Engineering, Shanghai Jiao Tong University, Xuhui, Shanghai 200030, China

[4] National Digital Manufacturing Technology Center and School of Biomedical Engineering, Shanghai Jiao Tong University, Xuhui, Shanghai 200030, China

Introduction

Mandibular angle split osteotomy (MASO) is a popular and useful procedure used to treat prominent mandibular angles, achieving improved esthetic results for the patients. Usually, it is performed meticulously by plastic and reconstructive surgeons. In the majority of cases, an exact osteotomy plane is one of the most critical steps in the success of MASO, but it is time consuming and invasive. Therefore, this step should be performed carefully to avoid postoperative complications, such as neurosensory disturbance of the inferior alveolar nerve [1, 2], fractures [3, 4], and infection [5].

To avoid such disadvantageous results, some surgeons prefer to use augmented reality (AR) technology when performing MASO surgery. AR is a combination technique of virtual reality, real-time interaction, and three-dimensional (3D) display that is able to merge virtual medical images with real entity models. It provides surgeons with direct perceptions of crucial structures and assists in developing preoperational plans. AR is of particular value in plastic surgery due to the need to respect the risk structures.

AR technology has been applied in the surgical treatment of patients with complex craniofacial deformities [6–8] and in the performance of mandible osteotomy [9–11]. These procedures were performed by surgeons experienced in osteotomies. However, inexperienced plastic surgeons must undergo a long period of clinical training to obtain the professional skills needed to be a qualified doctor. And, notably, physiological trembling and fatigue of surgeons may induce complications [12, 13]. As an alternative, robot-assisted surgery can be done safely and with precision, is less invasive, and results in quicker healing times and lower complication rates. Using robots in surgery gives surgeons more control over surgical instruments and a better view of the surgical site. Robot use can reduce fatigue and naturally occurring hand tremors because surgeons do not need to stand throughout the surgery and do not tire as quickly. Thus, a self-developed and constructed robot based on AR was designed and built specifically for mandibular plastic surgery, with the goals of achieving safety requirements of MASO surgery. We believe our robot system can especially assist inexperienced plastic surgeons in learning to perform MASO well. In preparation for using the robot on humans, an animal experiment was performed by plastic surgeons in the clinic.

In this study, we aim to present the preliminary results of MASO surgery performed by inexperienced plastic surgeons using a self-developed and constructed robot based on AR.

Materials and Methods

Study Design

To obtain a precise osteotomy plane for clinical MASO, two living dog specimens were operated on by surgeons. The most frequent complication of MASO is nerve damage [13]. To prevent this problem, the mandibular branch of the facial nerve should be identified and protected from damage. Thus, CT scans of each dog skull were obtained by using an imaging device (Siemens Somatom Definition Edge, resolution 0.156 mm^2, slice thickness 0.2 mm). These digital data were then imported into Mimics CAD/CAM software (Materialise, Leuven, Belgium) to render a 3D virtual structure of each dog's skull, as shown in Fig. 1. Segmentation thresholds were defined qualitatively for each case.

To ensure the osteotomy plane, the mandibular angle was exposed by conducting a subperiosteal dissection. Then, five holes that hold a safe distance to the mandibular were made according to the clinical experiences of plastic surgeons in the literature [14, 15] (shown in Fig. 1a, b). The consecutive holes were connected using an oscillating saw to generate the osteotomy plane, as shown in Fig. 1c. All applicable institutional and/or national guidelines for the care and use of animals were followed.

Surgical Robot Technique

The MASO procedures were performed by four plastic surgeons who had surgical expertise and familiarity with robot operation, using the proposed robot system. Force feedback is essential for the surgeons in the MASO operation. Generally, inexperienced surgeons need a lot of practice to learn how to control the unstable contacts and cutting motions involved in the manipulation of instruments with high-speed reciprocation or rotation. And we did not discussed it in previous work [10]. Thus, a force feedback control strategy is particularly important; this strategy assists in determining whether the drill bit will penetrate the bone or damage the nerve. According to the anatomical characteristics of the mandibular bone, the density differs from the internal to the external (from the cortical bone to the cancellous bone to the cortical bone). There are many bone gaps in the cancellous bone that will generate noise during the drilling procedure. To deal with this issue, an effective method of monitoring the drilling position was developed to determine whether the drill has broken through the bone. Thus, the strategy is that if the force value drops to zero after two peaks appear, the drilling will stop immediately. The workflow is as follows: let's define F_n and F_{n+1} as the force of the time n and $n+1$. First, if$\Delta F_n = F_{n+1} - F_n \leq 0$, the drill bit did not

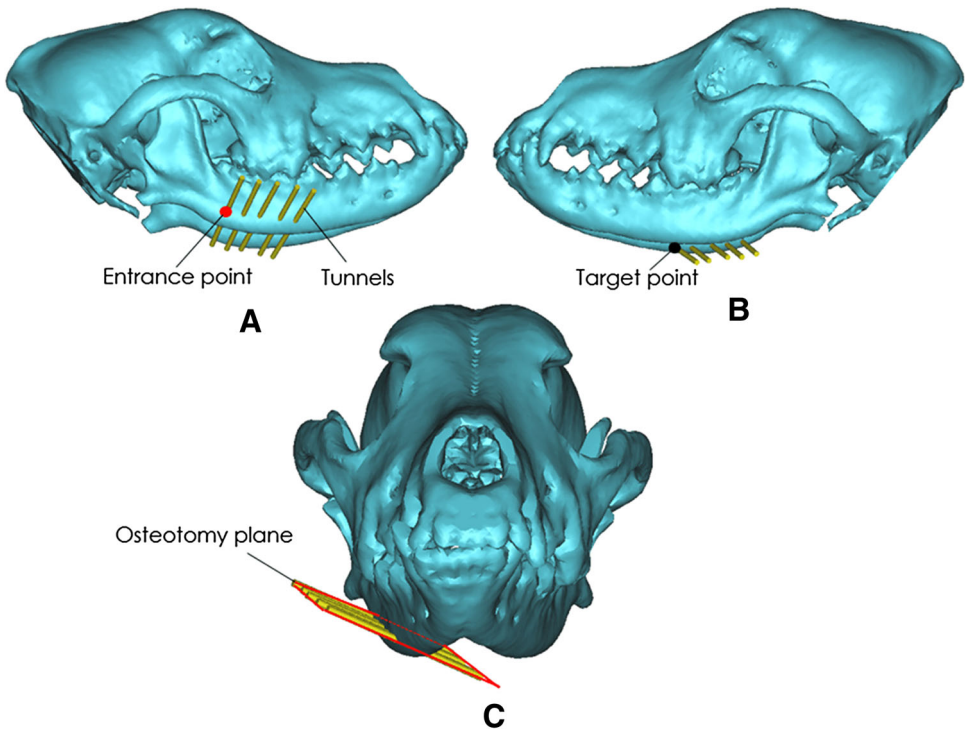

Fig. 1 Preoperational design of the drilling procedure **a** right view. **b** Left view. **c** Front view. The 3D dog model was reconstructed from the CT images. The *red point* in (**a**) is the entrance point of drilling. The *black point* in (**b**) is the target point of drilling. The *yellow cylinder* is the drilling tunnels. The *red plane* is the planned osteotomy plane. The *black dotted arrow* is the cutting direction

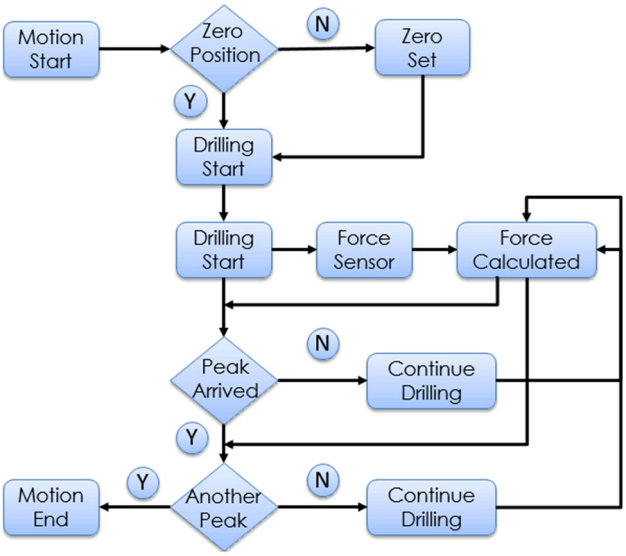

Fig. 2 Control flow chart of the force feedback strategy

drill into the bone; when $\Delta F_n = F_{n+1} - F_n > 0$, the drill bit drills into the external layer of the cortical bone; if $\Delta F_n > 0$ and $\Delta F_{n+1} < 0$, the peak of bone density occurs. Then, the drill bit will gradually penetrate the cortical bone when $\Delta F_{n+2} \leq \alpha$ (threshold value) occurs. Next, the drill bit drills into the cancellous bone. Similarly, if the peak value appears twice, we believe the drilling procedure has been completed, and it should be stopped immediately. The control flowchart is shown in Fig. 2.

The whole surgical robot system consists of two parts: the AR navigation system and the robot system (shown in Fig. 3). The AR navigation system consists of the tracking module, the operational system module, and the display module. The tracking module that we use is composed of the Micron Tracker system (Claron Company, Canada) and the registering marker [11]. The operational system module and the display module we used were AR Toolkits (AR Toolworks, Seattle, WA) and nVisor ST60 (NVIS Company, USA), separately. By using the AR navigation system, a preoperative surgical plan that created an exact osteotomy plane was achieved. This system also provided good guidance, particularly for inexperienced surgeons, in teaching them how to make the right decisions for MASO surgery.

Accordingly, the main component of the robot is a seven degree-of-freedom serial arm (shown in Fig. 4a), which is optimized by means of the gross weight (approximately 9.5 kg) and length (85 cm). It is mainly composed of five components: the support module, the position control module, the attitude control module, the motor module, and the end-effector module. All modules are manufactured of aluminum alloy. This not only ensures the strength and stiffness of the robot, but also reduces the overall weight. The kinematic design has a large workspace and allows effective intervention during the operation. A built-in force sensor (JHBM-M, JinNuo, China) at the end-effector provides an intuitive haptic interaction, which allows the surgeons to perceive the desired force feedback

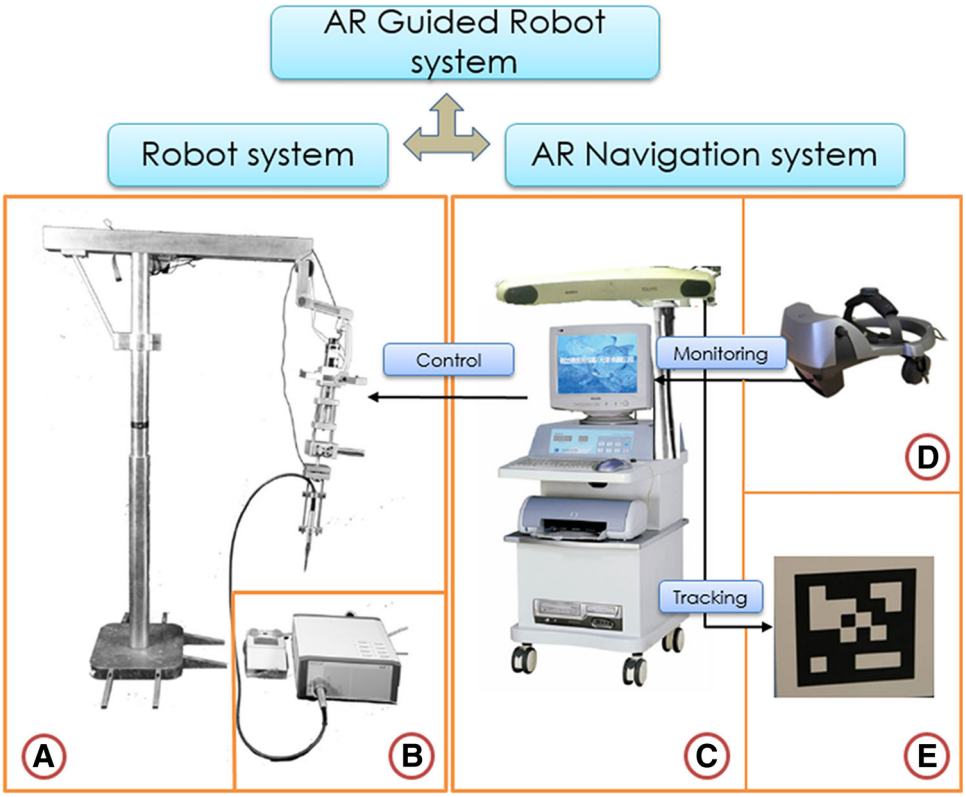

Fig. 3 Architectural structure of the robot system based on AR. *a* Mechanical structure; *b* power system of the drilling tool; *c* Micron Tracker and AR Toolkits system; *d* HMD system; *e* registration marker. The Micron Tracker identifies the marker's position in real time and sends the virtual information to the AR Toolkits system at the computer work station as well as the HMD system. Meanwhile, the real environment information is also collected by the cameras of the Micron Tracker. Afterward, the AR Toolkits system reconstructs 3D images and depicts them in HMD. By merging the virtual and actual images together, surgeons can perform the operations with the assistance of robot system by monitoring the HMD without switching to the computer screen

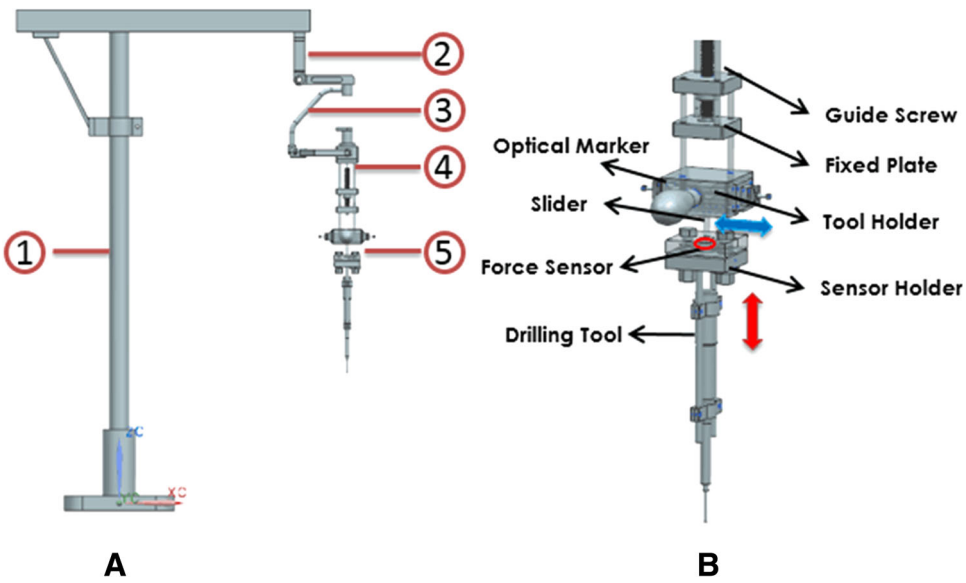

Fig. 4 Design of the mechanical structure system. **a** The robot is mainly composed of five components: the support module (*1*), the position control module (*2*), the attitude control module (*3*), the motor module (*4*) and the end-effector module (*5*); **b** force feedback mechanism

information during the surgery. As shown in Fig. 3b, the proposed force feedback mechanism mainly contains a guide screw, fixed plates, a tool holder, a slider, a sensor holder, a force sensor, and a drilling tool. When the guide screw is rotated by the motor, it translates the rotational motion of the guide screw into translational motion and pushes the fixed plate going down. At the same time, other parts connected with the fixed plate are moving along with the axial of the guide screw (shown as by the red arrow in Fig. 4b). Once the drilling tool is drilled into the bone, the force sensor generates a series of signals that can assist the doctor in monitoring the process and determining the safety of the surgery. The robot is linked by two cables to a controller device far away from the sterile field.

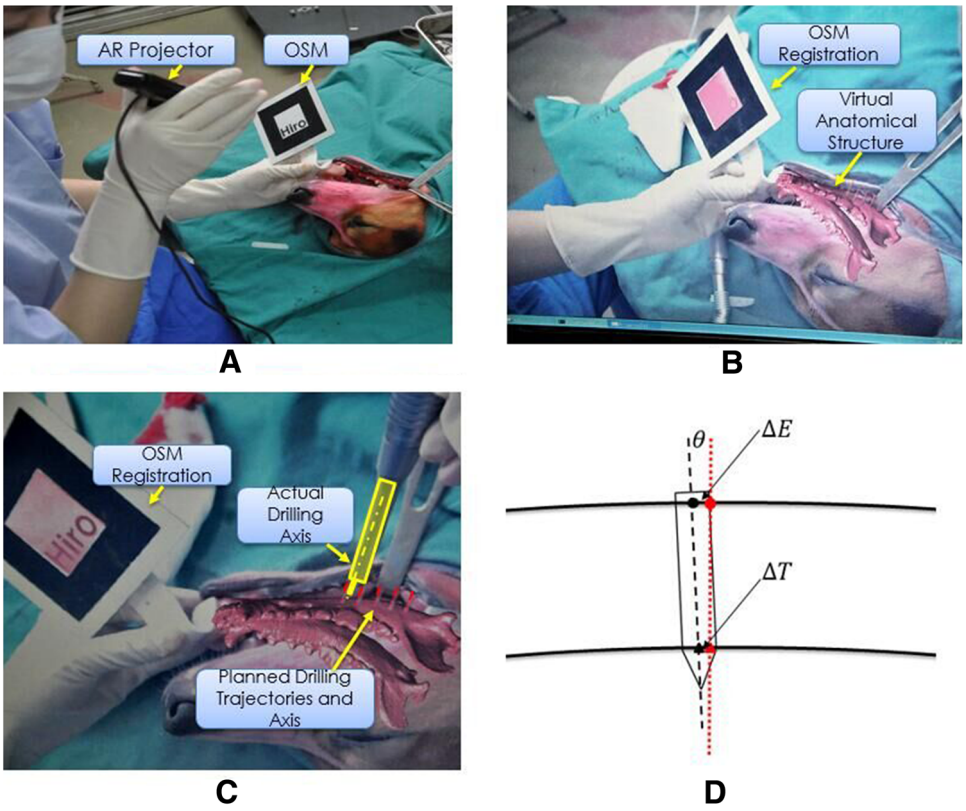

Fig. 5 Drilling procedure on animal test. **a** Preparing for registration. OSM must be steadily fixed, and virtual information should be preoperatively planned in this section. **b** Successful registration case. Virtual anatomical structure can be clearly seen overlapping with the actual mandible region in the computer screen. **c** Drilling accuracy evaluation with fusion of virtual information and actual information; **d** schematic diagram of accuracy evaluation. The *red dotted line* and *point* are the planed drilling axis and entrance/target point, respectively. The *black dotted line* and *point* are the actual drilling axis and entrance/target point, respectively. Where θ is the angular error, ΔE is defined as the entrance error, and ΔT is the target error

Robotic Surgery

Each dog specimen was under general anesthesia and fixed on the operating room table with sterilized clamping instruments. All preoperative sterilization of surgical instruments was completed. The mandibular bone region of the dog was then registered with the virtual images by digitizing the registering marker, as shown in Fig. 5a. Finally, the mandibular bone region was exposed in preparation for robot drilling.

Before robot drilling, the mandibular structures, including five virtual drilling tunnels preoperatively reconstructed for the dog, were prepared in the navigation system. Surgeons used the AR projector to overlap the virtual mandibular region information (including the virtual structures and the drilling tunnels) with the actual mandibular region of the dog, as shown in Fig. 5b. By changing the transparency settings of the display modality, a "see-through" effect was obtained. This effect assisted the surgeons in performing the operation. The actual drilling procedure was performed along the axis of the virtual tunnels by four inexperienced surgeons, as shown in Fig. 5c.

The osteotomy plane was obtained in two steps. First, a short, stiff spiral drill (Φ2.5 mm × 5 mm) was used to create a starter hole with a depth of 0.5 mm. This minimizes the deflections caused by off-normal lateral drilling forces. After the first starter hole was completed, others were obtained by moving the slider in the tool holder (shown as a blue arrow in Fig. 4b). Then, the first full-depth tunnel was drilled using a Φ2 mm × 25 mm spiral drill. Rotating at 5000 rpm and advancing at 0.5 mm/s, the tool was cooled constantly during drilling. Other tunnels were made according to the first tunnel. Finally, the osteotomy plane was obtained by cutting along all the tunnels, as shown in Fig. 6.

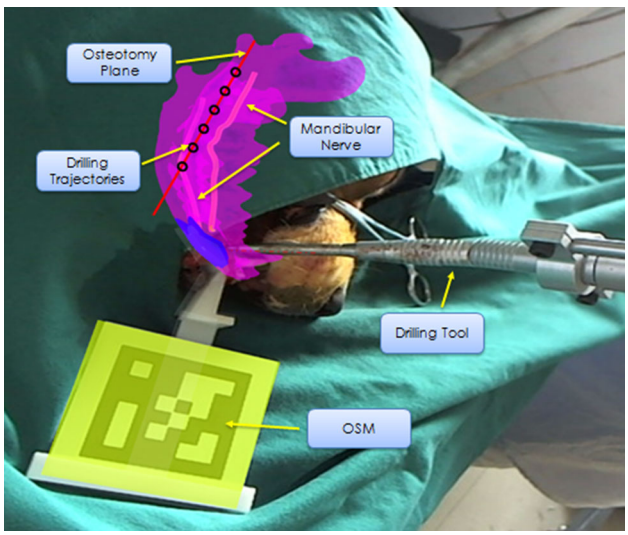

Fig. 6 Robot drilling of animal experiment in the operation room

Postoperative Analysis

Postoperative CT scans of mandibular region tunnels were acquired and compared with preoperative CT scans used to evaluate the accuracy of the MASO surgery. The Euclidian distances to the entrance/target points and mandibular nerve were evaluated. The technical accuracy includes the entrance/target error and the angular error (excluding depth error). The angular error was defined as the lateral deviation between the actual drilling axis and the planning drilling axis, as shown in Fig. 5d. All the errors were calculated utilizing the software MATLAB (The Mathworks Inc., USA).

Results

Four osteotomy planes were successfully performed; that is, twenty tunnels (each dog drilled on bilaterally) were drilled in the dogs' mandible bones. Both dogs recovered after 5 weeks, and the postoperative complications were observed.

The accuracy of the osteotomy plane includes the entrance/target error and angular error. Errors at entrance and target points were 1.04 ± 0.19 and 1.22 ± 0.24 mm, respectively (Table 1). Distances to the mandibular nerve are also reported as the absolute distance postoperatively. The angular error between the planned and drilled tunnels was 6.69° ± 1.05°. The time required for drilling each specimen was 21 ± 12 min. Initial trials required more than 45 min, but the time decreased with increased experience.

The safety requirement of the surgery is shown in Fig. 7, which is the result of the force feedback information. Of twenty tunnels, six cases were randomly chosen and analyzed. Two peaks of force feedback were observed in each case, which indicated that the full-depth drilling procedure was finished. These cases exhibited no visible damage to the mandibular nerve.

Table 1 Specific data of effective drilling accuracy measured

Specimen ID	Trajectory ID	Error (mm)		Angle (°)	Distances (mm)	Time (min)
		Entrance	Target		FN (actual/planned)	
S1-Left	1	1.24	1.35	6.79	7.09/5.00	3.5
	2	0.96	1.09	5.59	5.66/5.00	4.1
	3	1.56	1.89	8.65	7.45/5.00	3.8
	4	1.14	1.06	6.14	6.88/5.00	4.0
	5	0.88	1.05	5.23	4.89/5.00	3.6
	Mean ± SD	1.15 ± 0.27	1.29 ± 0.36	6.48 ± 1.35	6.39 ± 1.08	3.80 ± 0.25
S1-Right	1	0.81	0.98	5.09	5.47/5.00	4.4
	2	0.79	0.92	5.71	4.64/5.00	3.2
	3	1.06	1.26	6.59	6.87/5.00	3.6
	4	1.18	1.45	8.12	7.80/5.00	3.7
	5	0.93	0.98	7.89	6.32/5.00	4.0
	Mean ± SD	0.95 ± 0.17	1.12 ± 0.23	6.68 ± 1.32	6.22 ± 1.22	3.78 ± 0.45
S2-Left	1	0.93	1.07	7.78	7.17/5.00	3.7
	2	1.22	1.55	6.84	7.05/5.00	4.0
	3	1.09	1.37	5.71	6.51/5.00	3.8
	4	0.97	1.14	5.83	5.31/5.00	3.5
	5	1.03	1.02	7.34	4.81/5.00	3.6
	Mean ± SD	1.05 ± 0.11	1.23 ± 0.22	6.70 ± 0.91	6.17 ± 1.06	3.72 ± 0.19
S2-Right	1	0.82	1.05	7.91	7.88/5.00	3.8
	2	0.92	1.14	7.52	4.65/5.00	3.6
	3	1.21	1.43	6.91	6.93/5.00	4.0
	4	1.11	1.27	5.85	6.75/5.00	4.1
	5	0.95	1.35	6.44	5.89/5.00	4.0
	Mean ± SD	1.00 ± 0.16	1.25 ± 0.15	6.93 ± 0.82	6.42 ± 1.22	3.90 ± 0.20
Total	Mean ± SD	1.04 ± 0.19	1.22 ± 0.24	6.69 ± 1.05	6.30 ± 1.06	3.80 ± 0.28

S1-Left means drilling the left side of the first dog specimen, and others follow. Five trajectories of each dog were chosen for postoperative evaluation; facial nerve (FN)

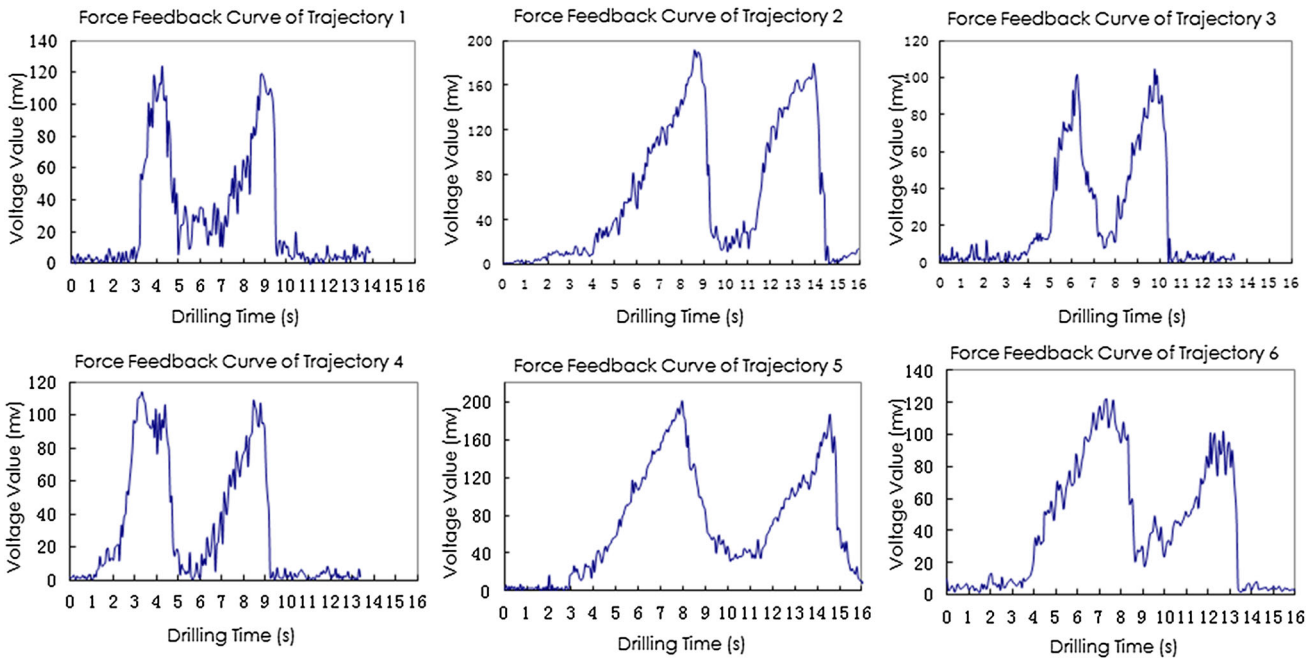

Fig. 7 Force feedback results of the six drilling trajectories

Table 2 Complication rates of the proposed technique performing MASO

Complications	$N = 4$
Hematoma	None
Deviation of the corner of the mouth	None
Injury to soft tissue in the mouth	None
Infection	None
Mandible fracture	None
Skin dehiscence	1
Nerve damage	None

When we evaluated the complications, one dog developed dehiscence of the head skin because of a very tight headband. No dogs experienced severe complications such as surgical infection, hematoma, or injury to soft tissues in the mouth. No obvious deviation at the corner of the mouth or fracture was observed in dogs with this technique (Table 2).

Discussion

The goal of MASO is to treat patients with mandibular hypertrophy who regard an oval face as attractive. Postoperative complications, such as mandible fracture and nerve damage [16], can be largely preventable by meticulous and precise surgical planning. Zhang et al. [17] reported that the intra/extraoral approach of MASO had few complications. The extraoral approach provides better visibility in the operation field and is easily operated, but it leaves scarring on the face. The intraoral approach is less invasive and requires less time than the extraoral approach [18]. However, the inability to see anatomical structures and the potential for naturally occurring hand tremors make the MASO procedure problematic. Thus, one of the most critical steps is to obtain a precise osteotomy plane, which is prone to complications when performed improperly.

In a review of the literature, Adamo and Azal [19] reported major complications (68.8% of the 32 patients) in mandibular reconstructive surgery. Moreover, the surgery often required expensive and complex medical care [20]. Recent advances in plastic surgery include preoperative planning [6–8, 21], surgical assistance [10, 22], and AR technology, with the latter attracting a lot of attention from researchers. AR has already been widely applied in many fields, including orthopedics, urological surgery, dentistry, ear–nose–throat surgery, and neurosurgery [22–26]. Thanks to the advantages of AR, surgeons can make precise preoperational plans and avoid crucial structures intraoperatively. Using a robot in surgery reduced complications [27] and resolved the problem of hand trembling and fatigue in surgeons. However, for inexperienced surgeons, it is impossible to implement this technology without a lot of training and practice.

In our technique, we have used both the AR technique and robotics. The burring and hole-connecting technique proposed in the literature [15] was used to meet safety requirements. As shown in Table 1, we measured the entrance/target

error instead of position error in the previous work for the purposes of evaluating the accuracy of the robot system and the surgeons' operation. The entrance error is related to the robot system, whereas the target error tends to be affected by the operation of the surgeon. Overall, the position error obtained in this study (Table 1) is comparable to our previous work and better than manual operation [10], indicating that this technique is helpful to inexperienced plastic surgeons who are performing MASO surgery. The entrance error ranges from 0.97 to 1.56 mm. There are two main sources of error: One originates from the inherent error of the robot system, and the other is the unsteady fixture of the dog. The target error ranges from 0.92 to 1.89 mm, indicating that surgeon hand trembling still affects the accuracy of the operation but not as much as manual operation. The angle error was a little higher than that reported in the present study, but it was safe in our experiment. Based on the planned and actual distances, we believe our technique was safe because no complications occurred (Table 2).

In investigation of the robot system, safety is another aspect that must be considered. The ability to monitor and control the robot system during MASO surgery should eliminate complications such as nerve damage or damage to soft tissue. As shown in Fig. 7, the results show that each force feedback drilling curve has two peaks, which means the mandibular bone is fully penetrated. The robot must be stopped immediately when the second peak occurs. However, there is a significant fluctuation after the second peak in curves 1, 4, and 6. This is due to the secondary cutting between the drill bit and the residual bone. The haptic feedback of our robot system enhanced the surgeons' perceptions of being in real surgical environments and assisted in training inexperienced surgeons. This also proves the safety of MASO surgery. In short, this technique provides many advantages: (1) It allows for precise preoperative planning for surgeons; (2) it allows for accurate surgical operation for a precise osteotomy plane; (3) it can be easily equipped, sterilized, and operated in the clinical setting; and (4) it is valuable in training inexperienced surgeons.

However, this technique also has limitations. First, although the robot system is suitable for MASO surgery, it may not be appropriate for more complicated plastic surgery due to there being fewer manipulation modules and less accuracy. The operators of this experiment are inexperienced surgeons who have professional knowledge of plastic surgery, but little clinical practice, and who underwent 2 weeks of robot operation training. In fact, the surgeons actually agreed to extend the training time because they sometimes misused the robot system. Friendly human–computer interaction needs further improvement. Second, the number of people and animals involved in this study should be appropriately increased to better measure the accuracy of the operation and the performance of the robot system. Third, more research on the potential thermal damage to the mandibular nerve as a result of drilling needs to be conducted, and this is likely to be further investigated in future studies. The optimization of the surgical procedures should be factors in reducing complex medical expenses. Future surgical evaluation should take into account the accuracy of the operation, cost, time, and probability of complications.

Conclusions

In this study, our robot system based on AR promises a precise osteotomy plane even when operated by inexperienced plastic surgeons. This technique can be regarded as a useful approach for training surgeons with various levels. We are confident that improvements in our technique will be able to meet the necessary accuracy and safety goals of more complex maxillofacial plastic surgeries.

Acknowledgements The work described in this paper was financed by National Natural Science Foundation of China (Nos. 61190124, 61190120, 81372097), The project of Science and technology commission of Shanghai municipality (Nos. 14441900800, 14441900802, 14DZ1941100, 14DZ1941103, 13DZ0511000), National Key Technology Support Program (No. 2009BAI71B06), National High Technology Research and Development Program of China (Nos. 2015AA043203, 2006AA01Z310, 2009AA01Z313), National Natural Science Foundation of China (Nos. 61311140171, 60873131), Project of SJTU Medical and Engineering Cross Fund (YJ2013ZD03, YG2012MS54). Shanghai Municipal Education Commission—Gaofeng Clinical Medicine Grant Support (20161420).

Compliance with Ethical Standards

Conflict of interest None.

Ethical Approval All applicable institutional and/or national guidelines for the care and use of animals were followed.

References

1. Macintosh RB (1981) Experience with the sagittal split osteotomy of mandibular ramus: a 13 year review. J Oral Maxillofac Surg 9(3):151–165
2. Al-Bishri A, Barghash Z, Rosenquist J, Sunzel B (2005) Neurosensory disturbance after sagittal split and intraoral vertical osteotomy: as reported in questionnaires and patients' records. Int J Oral Maxillofac Surg 34(3):247–251
3. Han K, Kim J (2001) Reduction mandibuloplasty: ostectomy of the lateral cortex around the mandibular angle. J Craniofac Surg 12(4):314–325
4. Hong SO, Ohe JY, Lee DW (2014) Salvage of the condylar fracture: complication management of mandibular angle ostectomy. J Craniofac Surg 25(6):582–584
5. Davis CM, Gregoire CE, Steeves TW, Demsey A (2016) Prevalence of surgical site infections following orthognathic surgery: a retrospective cohort analysis. Int J Oral Maxillofac Surg 74(6):1199–1206

6. Qu M, Hou Y, Xu Y, Shen C, Zhu M, Xie L, Wang H, Zhang Y, Chai G (2015) Precise positioning of an intraoral distractor using augmented reality in patients with hemifacial microsomia. J Craniofac Surg 43(1):106–112
7. Kapoor S (2015) Re: effectiveness of a novel augmented reality-based navigation system in treatment of orbital hypertelorism. Ann Plast Surg 77(3):662–668
8. Ricciardi F, Copelli C, Paolis LTD (2015) A pre-operative planning module for an augmented reality application in maxillo-facial surgery. Salento Avr 9254:244–254
9. Hou Y, Zhu M, Chai G, Zhang Y, Xu YR, Shen CC, Qu M (2013) Experimental study of mandible osteotomy guided by augmented reality. J Tissue Eng Reconstr Surg
10. Lin L, Shi Y, Tan A, Bogari M, Zhu M, Xin Y, Xu HS, Zhang Y, Xie L, Chai G (2016) Mandibular angle split osteotomy based on a novel augmented reality navigation using specialized robot-assisted arms—a feasibility study. J Craniofac Surg 44(2):215
11. Zhu M, Chai G, Zhang Y, Ma X, Gan J (2011) Registration strategy using occlusal splint based on augmented reality for mandibular angle oblique split osteotomy. J Craniofac Surg 22(5):1806–1809
12. Hwang K, Han JY, Kil MS, Lee SI (2002) Treatment of condyle fracture caused by mandibular angle ostectomy. J Craniofac Surg 13(5):709–712
13. Yamauchi K, Takahashi T, Kaneuji T, Nogami S, Yamamoto N, Miyamoto I, Yamashita Y (2011) Risk factors for neurosensory disturbance after bilateral sagittal split osteotomy based on position of mandibular canal and morphology of mandibular angle. J Oral Maxillofac Surg 70(2):401–406
14. Yang J, Wang L, Xu H, Tai N, Fan Z (2009) Mandibular oblique ostectomy: an alternative procedure to reduce the width of the lower face. J Craniofac Surg 20(8):1822
15. Jong Lim P, Hyun OC, Kun H, Chul Gyoo P (2014) Burring and holes connecting ostectomy for the correction of prominent mandible angle. J Craniofac Surg 25(3):1025–1027
16. Deguchi M, Iio Y, Kobayashi K, Shirakabe T (1997) Angle-splitting ostectomy for reducing the width of the lower face. Plast Reconstr Surg 99(7):1831
17. Zhang Y, Fang J, Zou L, Dai C, Zhu G, Feng S, Jin YQ, Lu MJ, Wang W, Qi ZL (2006) Lower face remodeling by mandibular angle ostectomy. Eur J Plast Surg 29(2):67–71
18. Nordin T, Nyström E, Rosenquist J, Astrand P (1987) Extraoral or intraoral approach in the oblique sliding osteotomy of the mandibular rami? Clinical experience and results. J Craniofac Surg 15(5):233
19. Adamo AK, Szal RL (1979) Timing, results, and complications of mandibular reconstructive surgery: report of 32 cases. J Oral Surg 37(10):755–763
20. Kroll SS, Schusterman MA, Reece GP (1992) Costs and complications in mandibular reconstruction. Ann Plast Surg 29(29):341
21. Hwang K, Han JY, Kil MS, Lee SI (2002) Treatment of condyle fracture caused by mandibular angle ostectomy. J Craniofac Surg 13(5):709–712
22. Gruber RM, Merten HA, Schliephake H (2005) Orthognatic surgery of the mandible with an ultrasonic bone cutting device. Int J Oral Maxillofac Surg 34(5):91
23. Borgmann H, Rodríguez SM, Salem J, Tsaur I, Gomez RJ, Barret E, Tortolero L (2016) Feasibility and safety of augmented reality-assisted urological surgery using smartglass. World J Urol 1–6
24. Bruellmann DD, Tjaden H, Schwanecke U, Barth P (2013) An optimized video system for augmented reality in endodontics: a feasibility study. Clin Oral Invest 17(2):441–448
25. Lapeer RJ, Chios P, Alusi GH, Linney AD, Davey MK, Tan AC (2000) Computer assisted ENT surgery using augmented reality: preliminary results on the CAESAR project. Lect Comput Sci 1935:849–857
26. Inoue D, Cho B, Mori M, Kikkawa Y, Amano T, Nakamizo A (2013) Preliminary study on the clinical application of augmented reality neuronavigation. J Neurol Surg A Cent Eur Neurosurg 74(2):71–76
27. Pugin F, Bucher P, Morel P, Bucher P, Morel P (2011) History of robotic surgery: from aesopand zeusto da vinci. J Vis Surg 148(5):e3–e8